Arabian Journal of Chemistry (2015) 8, 771–779

King Saud University

Arabian Journal of Chemistry

www.ksu.edu.sa
www.sciencedirect.com

ORIGINAL ARTICLE

Polyaniline nanocomposites *via in situ* emulsion polymerization based on montmorillonite: Preparation and characterization

M.A. Abd El-Ghaffar [b], A.M. Youssef [a,*], A.A. Abd El-Hakim [a]

[a] *Packing and Packaging Materials Department, National Research Centre, Dokki, Cairo, Egypt*
[b] *Polymers and Pigments Department, National Research Centre, Dokki, Cairo, Egypt*

Received 2 September 2013; accepted 4 January 2014
Available online 18 January 2014

KEYWORDS

Na^+-montmorillonite;
Polyaniline;
Polymer nanocomposites;
Exfoliation;
Intercalation

Abstract Polyaniline nanocomposites were prepared *via in situ* emulsion polymerization in the presence of Na^+ montmorillonite (Na^+MMT). For achieving this purpose the clay was organophilized to (MMT-CTA) form using cetyltrimethyl ammonium bromide (CTAB). The X-ray diffraction (XRD) demonstrated that the basal space of Na^+-montmorillonite increased after the organophilization from 11.21 to 19.35 Å. Polyaniline/montmorillonite (PAn/MMT) nanocomposites were prepared by intercalating the emulsion of aniline monomer with treated organically layers of (Na^+-MMT) using ammonium peroxydisulfate (APS) as an initiator. Furthermore aniline hydrochloride (AnHCl) was used as a modifier and monomer to prepare PAn/H^+MMT nanocomposites by cation exchange of the anilinuim moiety with the sodium ion inside the basal spaces which enlarged after the polymerization process to 35 Å as evidenced from X-ray diffraction (XRD). The d-spacing of the PAn/H^+-MMT nanocomposite was found to become wider about 23.79 Å than that of the pure Na^+-MMT, and successful intercalation or exfoliation of $PAnH^+$ into Na^+-MMT layers. The prepared PAn/MMT nanocomposites were characterized by thermal gravimetric analysis (TGA), scanning electron microscope (SEM), and transmission electron microscope (TEM). The electrical property measurements showed an enhancement in the conductivity values of the prepared nanocomposites especially on using AnHCl monomer to be in the order of 10^{-1} S/cm.

1. Introduction

Polyanilines have attracted much attention in view of scientific interest, easy availability of raw materials, simple and easy preparation path ways, light weight, good environmental stability, and resistance to corrosion and lower cost apart the added advantage that they can afford. Many articles were reported concerning various methods of preparation, character-

* Corresponding author. Tel.: +20 2 33322418; fax: +20 2 33370931.
E-mail address: amyoussef27@yahoo.com (A.M. Youssef).

Peer review under responsibility of King Saud University.

Production and hosting by Elsevier

1878-5352 © 2014 King Saud University. Production and hosting by Elsevier B.V. All rights reserved.
http://dx.doi.org/10.1016/j.arabjc.2014.01.001

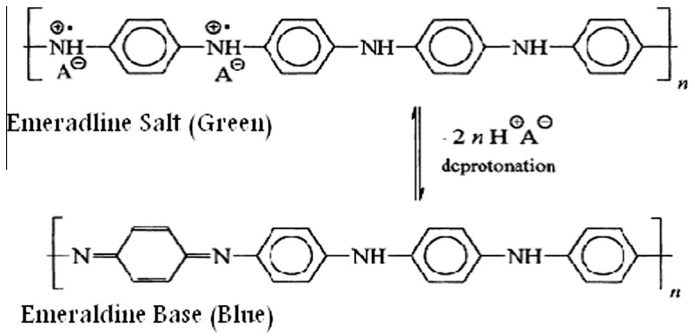

Scheme 1 Conducting PAn in the protonated emeraldine salt, (green color) as well as deprotonated in alkalis to the corresponding emeraldine base, which is blue and non-conducting.

izations and current commercial applications (Youssef et al., 2012a,b; Haroun and Youssef, 2011; Abd El-Ghaffar et al., 2006; Wazzan et al., 2005; Ismail et al., 1998; Chiang and MacDiarmid, 1986). The most promising and recent technological applications include fuel and solar cells (Jang et al., 2005), optical and microelectronic devices (Huang et al., 2003), sensors (Hosseini and Entezami, 2001), catalysts, drug delivery, energy storage systems, electrodes (Gharibi et al., 2006; Cao et al., 2002), photonic devices (Youssef et al., 2010) and packaging applications (Youssef, 2014).

However, PAn prepared in the inorganic acid media by chemical oxidation polymerization has some drawbacks, that it is inherently brittle and poor in process ability due to its insolubility in common organic solvents. The limited industrial applications of polyaniline (PAn) are due to its poor solubility (Inganäs and Lundström, 1987). The oxidation of aniline in acidic aqueous media using ammonium peroxydisulfate as oxidant has become the most widely used synthetic route to conducting PAn and is obtained as the protonated emeraldine salt, (green color). It is deprotonated in alkalis to the corresponding emeraldine base, which is blue and non-conducting (Scheme 1).

To overcome the process ability drawbacks of PAn by enhancing its solubility, Osterholm et al. (1993, 1994) have adapted emulsion polymerization route to prepare processable conducting polyaniline with good solubility, wherein aniline is

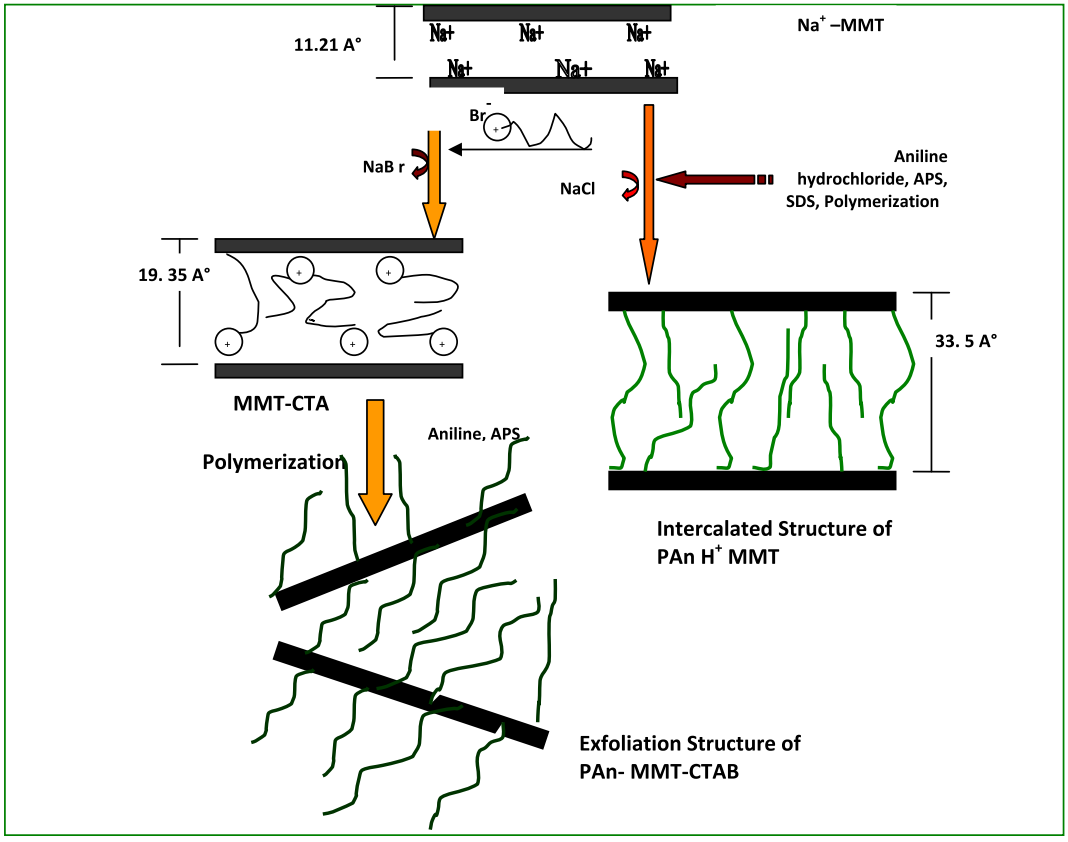

Scheme 2 Schematic represents the cation-exchange reaction between the montmorillonite and Cetyltrimethyl ammonium bromide as well as by *in situ* intercalative polymerization of aniline hydrochloride.

polymerized in an emulsion of water and a nonpolar or weakly polar organic solvent in the presence of dodecylbenzenesulfonic acid (DBSA) as protic acid & surfactant and ammonium peroxydisulfate as oxidant. Literature survey indicated that there are a lot of articles reporting thermoplastic and thermoset polymers/clay nanocomposites (Abdel Rehim et al., 2010; Porter et al., 1997; Faguy et al., 1994), while it is very poor about PAn/clay nanocomposites. By the way, the PAn/clay nanocomposites with different combinations of the two components have attracted more and more attention, since they have interesting physical properties and many prospective applications. The most widely utilized clay is the montmorillonite (MMT) for its large cation exchange capacity. On the other hand, PAn is not molten in nature and normally is insoluble in common solvents, on the other hand, clay particles are easily aggregated due to their high surface energy. The concept upon which nanocomposites were built, is based on conducting a polymerization process in the basal space of the clay, which is of a nanometric range (Youssef et al., 2013), consequently the preparation of PAn/clay nanocomposites by conventional blending or mixing in solution or melt form becomes very difficult. A number of methods have been used to prepare PAn/clay nanocomposite, the commonly used method to prepare the nanocomposite is the intercalation of aniline (aniline hydrochloride) into the gallery of clay layers followed by *in situ* polymerization (Kim et al., 2002; Nascimento et al., 2002; Leroux et al., 1997; Giannelis, 1996; Kerr et al., 1996; Allcock, 1992). Emulsion polymerization is also used for the preparation of PAn/clay nanocomposite (Bi et al., 2008; Ruiz-Hitzky et al., 1995) where the emulsifier in the emulsion system contributes to maximization of the affinity between hydrophilic host (clay) and hydrophobic guest (aniline). By the way, PAn/clay nanocomposite may open an approach to construct novel organic–inorganic hybrid systems showing electrical conductivity as well as good physical properties (Biswas and Sinha Roy, 2001). Moreover, during the last decade, an extensive research attention was compensated by the synthesis and evaluation of polymer/Na^+-MMT nanocomposites through intercalative emulsion polymerization of different monomers like aniline, thiophene, and pyrrole as well as using diverse emulsifiers such as sodium dodecylsulfate (SDS) (Jeevananda et al., 2008) or cetyltrimethylammonium bromide (CTAB). Lately, Choi et al. (2001) constructed nanocomposite of polyaniline (PAn) based on Na^+-MMT clay by emulsion polymerization using dodecylbenzenesulfonic acid (DBSA) as an emulsifier and ammonium peroxydisulfate (APS) as an initiator. Kim et al. (1999) have used emulsion polymerization pathway to synthesize PAn/clay nanocomposite in which DBSA was used not only as dopant but also as an emulsifier. The ratio of clay to aniline was fixed as 15-wt%. The XRD study of PAn/clay nanocomposite revealed that PAn was doped with DBSA, also, the intercalation between Na^+-MMT layers and PAn–DBSA in the nanoscale level. Moreover, it was demonstrated that quasi one-dimensional changeable range hopping model affords the excellent fit for PAn/clay nanocomposite.

The present study is focusing on the synthesis of PAn/Na^+-MMT nanocomposites *via in situ* emulsion polymerization of aniline onto Na^+-MMT nanoparticles and characterizing their electrical properties. In addition, we intend to synthesize PAn/Clay nanocomposites by using aniline hydrochloride instead of aniline; this has triple functions as monomer, dopant, and modifier for Na^+-MMT. Moreover, we report that an intercalated PAn/Na^+-MMT nanocomposite without modification of Na^+-MMT is first prepared using *in situ* emulsion polymerization of aniline hydrochloride.

2. Materials and methods

2.1. Materials

Aniline (99% purity, Aldrich) was distilled under reduced pressure and stored at low temperature prior to use, aniline hydrochloride was obtained from Sigma Aldrich, cetyltrimethyl ammonium bromide (CTAB) and sodium dodecylsulfate (SDS) were provided by Merck, Darmstadt, Germany. Na-montmorillonite (MMT) with cation exchange capacity (CEC) of 90 mEq/100 g, under trade name Mineral colloid BP, was purchased from Southern Clay Products Inc. Ammonium peroxydisulfate (APS) and hydrochloric acid (HCl) were used as received from Alfa Aesar.

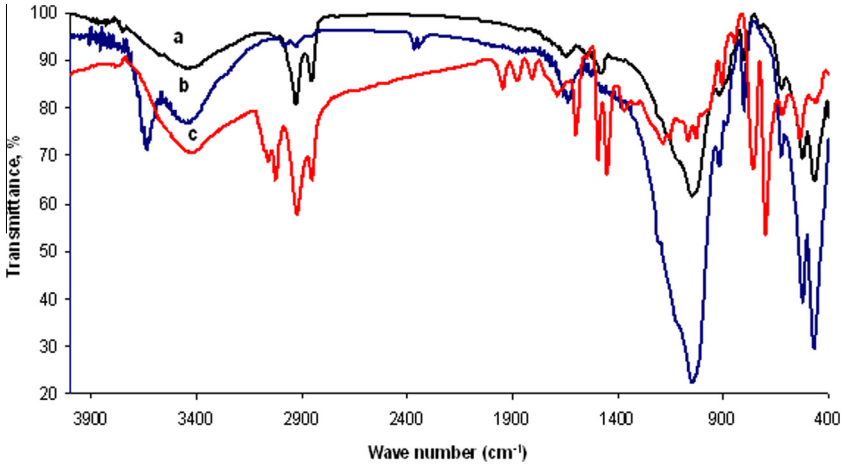

Figure 1 FTIR spectra nanocomposites of untreated (MMT) as well as treated montmorillonite (MMT-CTAB) and PAn/MMT-CTAB.

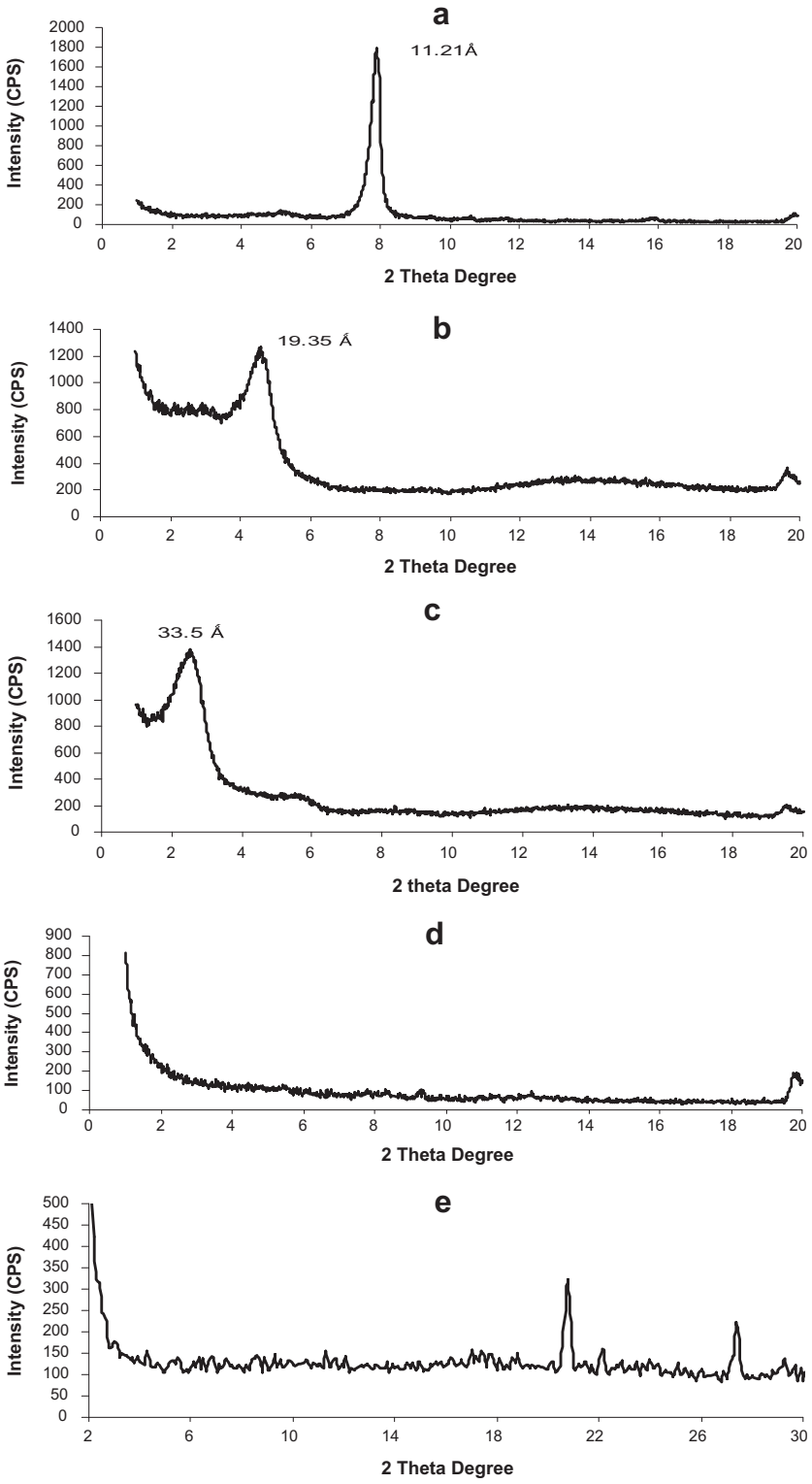

Figure 2 XRD of: (a) Na^+-MMT, (b) CTAB–MMT, (c) PAn–H^+MMT nanocomposites and (d) PAn/MMT-CTAB nanocomposites, (e) Pure PAn.

2.2. Modification of montmorillonite

Na^+-MMT clay was dispersed in water containing a stoichiometric amount of cetyltrimethyl ammonium bromide (CTAB) as a cationic surfactant, which causes complete cation exchange, at room temperature then the temperature was increased to 70 °C under vigorous stirring for 8 h. The weight ratio of the montmorillonite/water was 1/50. The clay was separated by filtration and washed several times with distilled water before vacuum dried at 60 °C for 24 h. Complete cation

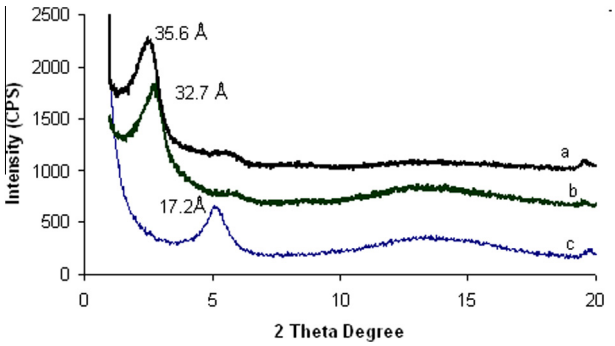

Figure 3 XRD of PAn nanocomposites prepared by emulsion polymerization for 6 h using aniline hydrochloride as monomer and using (0.2 M) of APS as initiator as well as (0.25 M) of SDS as surfactant with different Na^+-MMT contents, (a) 5%, (b) 10% and (c) 15%.

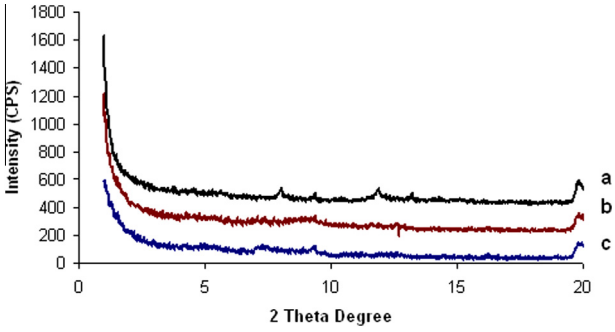

Figure 4 XRD of PAn/MMT-CTAB nanocomposites prepared by emulsion polymerization using different MMT-CTA concentrations, (0.2 M) APS as initiator for 6 h reaction times. (a) 5%, (b) 10% and (c) 15%.

exchange was confirmed on the filtrate by the addition of $AgNO_3$. Finally the clay was ground with a mortar and a pestle into fine powder. The abbreviation, MMT-CTAB refers to the treated montmorillonite with the cationic surfactants.

2.3. Synthesis of PAn/clay nanocomposite via in situ emulsion polymerization

The conducting nanocomposites of PAn/clay were prepared by emulsion polymerization. First an emulsion was formed using SDS (0.25 M) in water and chloroform with vigorous stirring. Various weight percentages of MMT-CTAB (5, 10, and 15 wt% based on the monomer concentration) were then dispersed in an emulsion. The aniline solution (0.2 M) was added to the above dispersion with steady stirring. Finally, the initiator solution of APS (0.25 M)/0.1 M HCl aqueous solution was added dropwise to the solution at 25 °C over a period of 30 min with constant stirring to initiate the polymerization of aniline. The reaction was continuous for 24 h at room temperature, in order to ensure the complete polymerization of aniline. Then, the polymerization was terminated by pouring the reaction mixture into acetone, at which the PAn/clay nanocomposites precipitated out. The PAn/clay was thoroughly washed with deionized water to eliminate the unreacted monomer, excess SDS, and finally washed with acetone.

2.4. Synthesis of PAn.HCl/clay nanocomposite via in situ emulsion polymerization

The same procedure was applied for the *in situ* emulsion polymerization of aniline hydrochloride (as monomer and modifier) using ammonium persulfate as oxidizing initiator in the presence of untreated montmorillonite and in the absence of SDS. The precipitated composite was thoroughly washed with

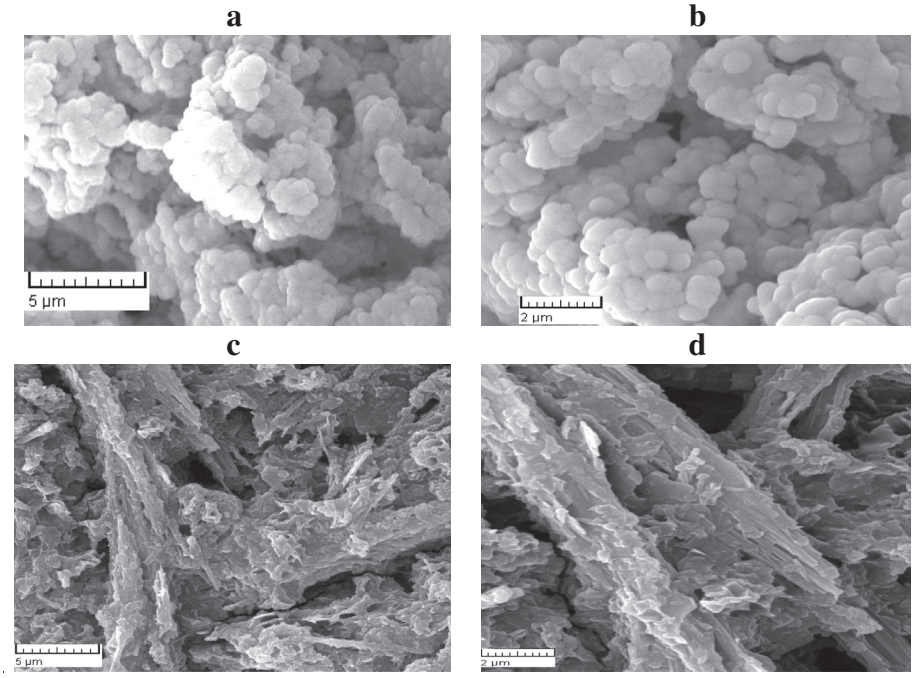

Figure 5 SEM images of Pure PAn (a, b) and PAn/clay nanocomposites (c, d).

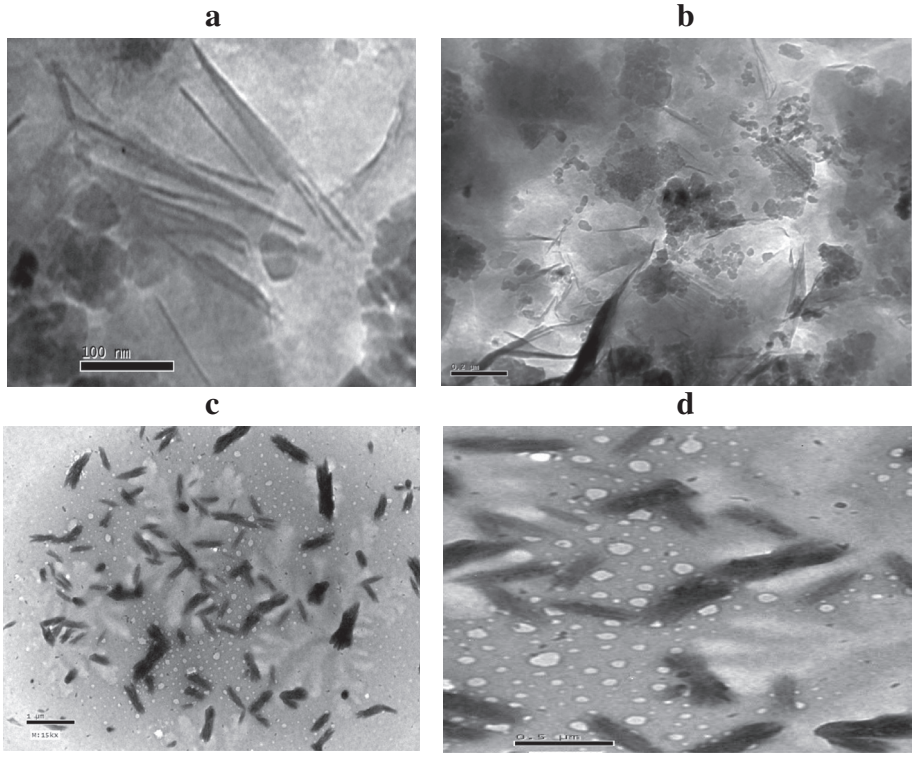

Figure 6 TEM images of (a, b) PAn/CTA-MMT nanocomposite and (c, d) PAn–H^+MMT nanocomposites.

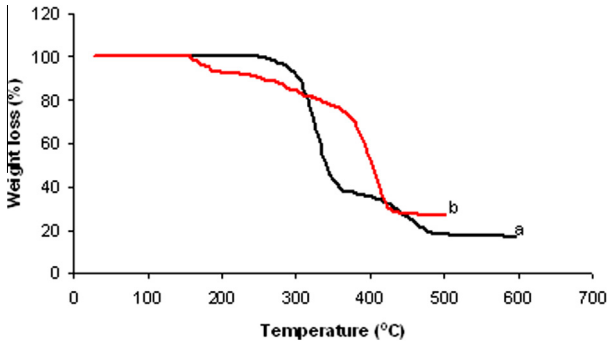

Figure 7 TGA curves of (a) Pure PAn and (b) PAn/H^+clay nanocomposite.

deionized water to eliminate the unreacted monomer, and finally washed with acetone; the powder was dried in a vacuum oven at 60 °C for 24 h.

2.5. Characterization

XRD (X-ray diffraction) patterns of the PAn/Na^+montmorillonite nanocomposites were measured on a Philips X-ray diffractometer (PW 1930 generator, PW 1820 goniometer) with CuK radiation source (λ = 0.15418 nm). The basal spacing (d_L) was calculated from the (0 0 1) reflection via Bragg's equation. The thermal stability was evaluated on a thermal gravimetric analyzer (TGA), Perkin Elmer using about 20 mg of the samples at a heating rate of 10 °C/min. under nitrogen atmosphere. The microstructure of the samples was examined for very dilute suspensions of the corresponding PAn/Na^+-montmorillonite nanocomposites in water using JEOL JEM-1230 transmission electron microscope (TEM) with acceleration voltage of 80 kV. The microscopy probes of the nanocomposites were prepared by adding small drops of the water dispersions onto a Lacey carbon film coated with copper grid and allowed to dry initially in air then by applying high vacuum. Also, scanning electron microscope (SEM), Tescan VEGA-II, USA, operated at 20 kV, was used for examining the clay layer morphologies and surface characters of the resulting nanocomposites. Fourier transforms infrared spectra (FTIR) of the sample powders were collected from KBr disks using a Nicolet, Nexus Spectrophotometer.

The molecular weight values and polydispersity of the prepared polyaniline were measured using a gel permeation chromatograph instrument (GPC) with THF as solvent and PS as standard using Agilent 1100 series, Germany, Detector: Refractive Index. Plgel particle size (5 μm), pore type (100, 104, 105 Å) on series, length 7.5 × 300 mm (1000, 500,000).

Table 1 The steps of weight losses at different temperatures.

	1st step	2nd step	3rd step
Pure PAn	300 °C % loss 10	350 °C % loss 70	500 °C % loss 87
PAn/H^+clay nano-composite	300 °C % loss 20	350 °C % loss 25	500 °C % loss 77

Table 2 AC conductivity (S cm^{-1}) at 25 °C of PAn–HCl as well as PAn–H^+MMT nanocomposites in dependence of frequency.

Frequency, Hz	3×10^6	1×10^6	5×10^5	2×10^5	1×10^5	5×10^4
PAn–HCl	14	13.8	13.4	13	12.5	12
PAn–H^+MMT, 5%	1.2×10^{-1}	1.1×10^{-1}	0.9×10^{-1}	0.7×10^{-1}	0.6×10^{-1}	0.5×10^{-1}
PAn–H^+MMT, 10%	1×10^{-1}	0.94×10^{-1}	0.78×10^{-1}	0.55×10^{-1}	0.04×10^{-1}	0.38×10^{-1}
PAn–H^+MMT, 15%	0.98×10^{-1}	0.92×10^{-1}	0.83×10^{-1}	0.53×10^{-1}	0.5×10^{-1}	0.37×10^{-1}

The AC conductivity measurements were carried out on disks, prepared by compression at room temperature, in the temperature range 30–120 °C at frequencies from 50 kHz and up to 5 MHz at maximum current 99 mA using Tioki 3531Z Hitester 131, Hioki E.E. Corporation-Japan.

3. Results and discussion

The exchange of Na^+-montmorillonite clay to the treated form by replacing the Na^+ with an organic cation is a key factor to improve the compatibilization between the inorganic clay and polymeric materials of this hybrid composite. This organic cation may be in the form of initiator, monomer or surfactant as in our case (CTAB) and this will lead to increase in the affinity of the Na^+-MMT to the organic phase and shows maximum swelling in the monomer due to the penetration of aniline between and onto the inter layer spaces of the clay, where it can interact inside with the permanent surfactant molecules by the hydrophobic-hydrophobic and Van Der-Waal interaction forces. For the given clay, the maximum amount of cations that can be taken up is constant and is known as the cation-exchange capacity [CEC]. It is measured in milliequivalents per gram [meq/g] or more frequently per 100 g [meq/100 g]. In the recent years an enormous number of polymer clay nanocomposites were fashioned. The polymers used included poly methyl methacrylate (Wazzan et al., 2005), and polystyrene (Wu et al., 2000) polyaniline (Youssef, 2014) while the most frequently used clay for this category of materials was montmorillonite because it can be easily intercalated with different kinds of modifiers (Youssef et al., 2013). In all cases and as a preliminary step (Youssef et al., 2010), the layered silicate (montmorillonite) must be converted to organic modified silicate by cation exchanging the sodium or the calcium with an organic modifier as shown in Scheme 2. It is obvious that CTAB can expand the basal space of montmorillonite from 11.21 to 19.35 Å; these data are consistent with that obtained by Tseng et al. Also, CTAB as a modifier acquired better regularity. Several reaction conditions were tried in order to optimize the different parameters of the polymerization process that provide enhanced properties if employed. In addition, there are two idealized polymer clay nanocomposites; intercalated and exfoliated ones. In the case of the exfoliated nanocomposites, the silicate layers of the clay became completely separated into individual layers of nanometer range. These layers are uniformly dispersed in the polymer phase in case of aniline prepared using modified clay (MMT-CTAB) (Youssef, 2014). On the other hand, extended polymer chains are intercalated between the silicate layers causing only expansion to the original silicate layers from 11.21 to 33.5 Å. The concept of conducting the polymerization process in the basal space of the clay which is of nanometric range, is based on initiating many growing polymer chains inside this very confined space which might at least expand this space (intercalation) in the case of using aniline hydrochloride with unmodified clay (Na^+-MMT).

3.1. The molecular weight (Mw)

The molecular weight (Mw) of the prepared polymer was estimated, using GPC with RI detector, after withdrawal of the clay layers from the PAn/clay nanocomposite and then measure the Mw which were found to be in the range of 6.8×10^3–8×10^3 g mol^{-1} with a polydispersity of 1.2.

3.2. FTIR spectra

The intercalation of CTAB was supported–proved by the recorded FTIR spectra (Fig. 1b). In addition to the characteristic peaks of Na^+-MMT, observed at 3630, 1036 and 465 cm^{-1} as shown in Fig 1a, which are ascribed to the OH stretching of the lattice water, Si–O and Al–O stretching, and Si–O bending, respectively, some new bands appeared in the case of MMT-CTAB at 1375 cm^{-1} (–CH_3), and 2900 cm^{-1} (–CH aliphatic). Also, the characteristic peaks of doped PAn are observed at 3400 cm^{-1} , attributed to N–H stretching mode, while bands appeared at 3050 cm^{-1} are assigned for the aromatic C–H stretching, while the bands at 1563, 1474, 1303, 1230, 804, and 518 cm^{-1}, corresponding to quinoid ring structure, benzenoid ring structure, and out of-plane bending, respectively (Fig. 1c), this peaks probably due to the physical interaction between PAn chains and silicate layers (Wazzan et al., 2005; Wu et al., 2000). This was evidenced as well from the X-ray pattern shown in Fig. 2. It is obvious that CTAB can expand the basal space of montmorillonite effectively.

3.3. The X-ray diffraction (XRD)

The X-ray diffraction (XRD) profile clearly shows that different basal spacings are arranged in a random fashion in the case of CTAB compared with PAn/clay nanocomposites which is likely to afford easier exfoliation or intercalation upon conducting the *in situ* polymerization. Several reaction conditions were tried in order to optimize the different parameters of the polymerization process that provide enhanced properties if employed. Moreover, X-ray diffraction (XRD) has often been used for determining the degree of intercalation and/or exfoliation of clay in the polymer matrix. When XRD patterns for pristine clay (Na^+-MMT), PAn/MMT-CTAB and PAnH^+-MMT nanocomposites are compared with each other, as shown in Fig. 2, the following facts are realized. First, the d-spacing of Na^+-MMT in MMT-CTAB increases from 11.21 Å in pristine clay to 19.35 Å, as shown in Fig. 2a and b, indicating that the surfactant molecules are intercalated into

the gallery of clay layers. Also, in the case of $PAnH^+$-MMT the PAn chains intercalated between the MMT layers by replacing the Na^+ and the polymerization process takes place between the clay layers which lead to increase in the basal spacing to 33.5 Å as revealed in Fig. 2c (intercalated). By carrying out the *in situ* oxidative polymerization of aniline in the occurrence of MMT-CTA form, most of clay layers are dispersed in the polymer matrix (exfoliated) as can be seen in Fig. 2d. Furthermore, for pure PAn, two peaks were observed at around $2\theta = 20°$ and 27°. The peak centered at $2\theta = 20°$ may be attributed to periodicity parallel to the polymer chain, while the peaks at $2\theta = 27°$ may be due to the periodicity perpendicular to the polymer chain (Kim et al., 2002).

Figs. 3 and 4 represent the X-ray diffraction patterns of some PAn–MMT nanocomposites prepared using MMT and MMT-CTA forms. It was found that the tendency for exfoliation is more pronounced in the case of MMT-CTA for the same concentration of the initiator; the d-spacing of MMT-CTA is greater than in the case of pristine clay so, it is thought to be making the reaction more favorable and leading to exfoliated nanocomposites by conducting MMT-CTA concentrations (5–15%) (Fig. 4a–c). On the other hand, when MMT was used without any modification, the tendency for intercalation is predominant (Fig. 3a–c). Furthermore, Fig. 3 demonstrated that by increasing the concentrations of the clay ratio from 5% to 15% the d-spacing decreases from 35.6 Å to 17.2 Å as the polymer contents necessary to cause the exfoliation and keeping the clay platelets away from each other are less.

3.4. SEM images

SEM images illustrated the formation of granular structure which is the most typical form for PAn prepared in the classic way in acidic aqueous media (Youssef, 2014) (Fig. 5a and b). The changes in the morphology are remarkable for the PAn/clay nanocomposites, an ill-shaped tubular like crust is now coating the surface of clay layers clearly (the rough part) as revealed in Fig. 6c and d.

3.5. TEM images

To more clearly identify exfoliated or intercalated structures of the PAn/clay nanocomposites, TEM images were done for the different nanocomposite formulations. It is clearly seen from Fig. 6, that the gray/white area represents the polymer matrix and dark stripes represent the clay layers. TEM images of PAn/MMT-CTA (Fig. 6a and b) confirm completely exfoliated structures, i.e., the clay layers are uniformly dispersed in the polymer matrix. Conversely, the TEM image of PAn–H^+MMT (Fig. 6c and d) shows that the prepared nanocomposite has a considerable amount of stacked layers in which polymer chains are intercalated, which is reliable with the results of X-ray diffraction (Figs. 3 and 4) respectively.

3.6. Thermal stability

The thermal stability of the pure PAn and the prepared PAn/clay nanocomposite do not show any significant weight loss up to 160 °C, and from 160 °C, up to 300 °C, pure PAn shows better thermal stability than PAn/clay nanocomposite. Starting from 300 °C, pure PAn showed sharp decomposition where it loses the majority of its weight, on contrast to PAn/clay nanocomposite which showed better thermal stability in this stage and retaining 70% of its initial mass up to 350 °C as can be seen from the thermograph illustrated in Fig. 7. Table 1 shows the different steps for thermal decomposition of pure polyaniline and PAn/clay nanocomposite which indicated that the $PAnH^+$/clay nanocomposite is more thermally stable, which is probably due to the attractive Columbic interaction between the positively charged nitrogen of the anilinium moiety and the negatively charged surface of the clay layer.

3.7. The AC conductivity

The conductivity values of PAn nanocomposites measured as pellets are given in Table 2. However, the AC conductivity, measured at a wide frequency range, remained temperature independent. The conductivity of the PAn nanocomposites is in the range of 0.05–0.12 S/cm. The higher conductivity of $PAnH^+$ obtained by the emulsion pathway could be due to a more homogenous protonation of the imine nitrogen of the anilinium moiety and more ordered chain conformation of the polymer (Youssef et al., 2012a, 2013). The conductivity of the PAn–MMT nanocomposites was found to be less than pure $PAnH^+Cl$, which shows higher conductivity values (12–14 S/cm).

4. Conclusion

Cetyltrimethyl ammonium bromide was used to organophilize the clay to prepare (MMT-CTA) form and the basal space increased after the organophilization from 11.21 to 19.35 Å. Furthermore, the basal space increased to 35 Å, when aniline hydrochloride was used to prepare PAn/H^+MMT nanocomposites as evidenced by X-ray diffraction. Successful preparation of exfoliated and intercalated (PAn)/clay nanocomposites *via in situ* emulsion polymerization pathway of aniline, aniline hydrochloride onto the layers of Na^+-montmorillonite. The XRD showed exfoliated and intercalated nanocomposites. The prepared nanocomposites exhibited better thermal stability as compared with pure polyaniline, and the conductivity of the prepared PAn–H^+MMT nanocomposites was found to be in the range of 0.037–0.120 S/cm with respect to average value of 12–14 S/cm that belongs to (emeraldine salt) PAn–HCl for a given frequency.

References

Abd El-Ghaffar, M.A., Mohamed, N.A., Ghoneim, A.A., Shaffei, K.A., 2006. Polym. Plast. Technol. Eng. 45, 1327–1338.
Abdel Rehim, M., Youssef, A.M., Hassan, E., Khatab, N., Turky, G., 2010. Synth. Met. 160, 1774–1779.
Allcock, H.R., 1992. Science 255, 1106–1112.
Bi, Z.H., Hung, Y.C., Liang, C., Yu, J.L., Ying, J.H., Po, H.T., Tar, H.H., Ko, S.H., 2008. Polymer 49, 4218–4225.
Biswas, M., Sinha Roy, S., 2001. Adv. Polym. Sci. 155, 167–221.
Cao, T., Wei, L., Yang, S., 2002. Langmuir 18, 750–753.
Chiang, J.C., MacDiarmid, A.G., 1986. Synth. Met. 13, 193–205.
Choi, H.J., Kim, J.W., Joo, J., Kim, B.H., 2001. Synth. Met. 121, 1325–1326.
Faguy, P.W., Ma, W., Lowe, J., Alan, J., Pan, W.P., Brown, T., 1994. J. Mater. Chem. 4, 771–772.

Gharibi, H., Zhiani, M., Entezami, A.A., Mirzaie, R.A., Kheirmand, M., Kakaei, K.J., 2006. Power Source 155, 138–144.
Giannelis, E.P., 1996. Adv. Mater. 8, 29–35.
Haroun, A., Youssef, A.M., 2011. Synth. Met. 161, 2063–2069.
Hosseini, S.H., Entezami, A.A., 2001. Polym. Adv. Technol. 12, 482–493.
Huang, J., Virji, S., Weiller, B.H., Kaner, R.B., 2003. J. Am. Chem. Soc. 125, 314–315.
Inganäs, O., Lundström, I., 1987. Synth. Met. 21, 13–19.
Ismail, M.N., Ibrahim, M.S., Abd El-Ghaffar, M.A., 1998. J. Polym. Degrad. and Stab. 62, 337–341.
Jang, J., Bae, J., Lee, K., 2005. Polymer 46, 3677–3684.
Jeevananda, T., Siddaramaiah, Nam, H.K., Seok-Bong, H., Joong, H.L., 2008. Polym. Adv. Technol. 19, 1754–1762.
Kerr, T.A., Wu, H., Nazar, L.F., 1996. Chem. Mater. 8, 2005–2015.
Kim, J.W., Kim, S.G., Choi, H.J., Jhon, M.S., 1999. Macromol. Rapid Commun. 20, 450–452.
Kim, B.H., Jung, J.H., Hong, S.H., Joo, J.S., Epstein, A.J., Mizoguchi, K., Kim, J.W., Choi, H.J., 2002. Macromolecules 35, 1419–1423.
Leroux, F., Goward, G., Power, W.P., Nazar, L.F., 1997. Electrochem. Soc. 144, 3886–3895.
Nascimento, G.M., Constantino, V.R.I., Temperini, M.L.A., 2002. Macromolecules 35, 7535–7537.
Osterholm, J.E., Cao, Y., Klavetter, F., Smith, P., 1993. Synth. Met. 55, 1034–1039.
Osterholm, J.E., Cao, Y., Klavetter, F., Smith, P., 1994. Polymer 35, 2902–2906.
Porter, T.L., Haggerman, M.E., Eastman, M.B., 1997. Recent Res. Dev. Polym. Sci. 11, 1–17.
Ruiz-Hitzky, E., Aranda, P., Casal, B., Galván, J.C., 1995. Adv. Mater. 7, 180–184.
Wazzan, A.A., Ismail, M.N., Abd El-Ghaffar, M.A., 2005. Int. J. Polym. Anal. Charact. 10, 57–69.
Wu, Q., Xue, Z., Qi, Z., Wang, F., 2000. Polymer 41, 2029–2032.
Youssef, A.M., 2014. RSC Adv. 4, 6811–6820.
Youssef, A.M., Abdel Rehim, M., Hassan, E., Khatab, N., Utilization of different conductive polymer systems in nanowires dye-sensitized solar cells, 43rd IUPAC world polymer Congress (Macro2010), 11–16 July 2010 Glasgow, UK.
Youssef, A.M., El-Samahy, M.A., Abdel Rehim, M., 2012a. Carbohydr. Polym. 89, 1027–1032.
Youssef, A.M., Elsamahy, M.A., Elsakawy, M., Kamel, S., 2012b. Carbohydr. Polym. 90, 1003–1007.
Youssef, A.M., Bujdosó, T., Hornok, V., Papp, S., Abdel Hakim, A., Dékány, I., 2013. Appl. Clay Sci. 77–78, 46–51.